Mühendislik Bilimleri ve Tasarım Dergisi
12(4), 835-847, 2024
e-ISSN: 1308-6693

Journal of Engineering Sciences and Design
DOI: 10.21923/jesd.1558750

Araştırma Makalesi Research Article

PERFORMANCE COMPARISON OF WINDING TYPES AND ROTOR STRUCTURE IN SYNCHRONOUS RELUCTANCE MOTOR

Emin Tarık KARTAL[1], Fatma KESKİN ARABUL[1*]

[1] Yildiz Technical University, Department of Electrical Engineering, Istanbul, Türkiye

Keywords

Electrical Machines, Synchronous Reluctance Motors, Winding Types, Rotor Barriers, Finite Element Analysis.

Abstract

Synchronous Reluctance Motors (SynRMs) have attracted a lot of attention in recent years due to their simple construction, high efficiency and the fact that they do not require rare earth magnets. SynRMs produce torque by directing the magnetic flux through barriers in the rotor, making them a low-cost alternative. The performance of the motor can vary significantly depending on the design of the stator windings and rotor barriers. Different combinations of stator winding types and the number of rotor barriers directly affect the critical performance parameters of the motor such as torque, efficiency, torque ripple, output power, saliency ratio and copper consumption. In this study, SynRMs using six different stator winding types and two different rotor barrier structures (3 and 4 barriers) are analyzed. Output power, efficiency, torque, torque ripple, saliency ratio, d-q axis inductances depending on current phase angle, total losses and copper consumption are investigated. The effect of full pitch and shortened pitch configurations in winding structures on the performance is discussed comparatively. The effect of 3 and 4 barrier rotors on these parameters is also evaluated. These analyses aim to reveal the ways in which winding and rotor configurations in motor design can be used to optimize performance. SynRMs can provide energy efficiency and cost benefits in a variety of industrial applications, therefore selecting the proper configuration is of great importance from both an economic and performance perspective.

SENKRON RELÜKTANS MOTORDA SARGI TİPLERİNİN VE ROTOR YAPISININ PERFORMANS KARŞILAŞTIRMASI

Anahtar Kelimeler

Elektrik Makinaları, Senkron Relüktans Motorlar, Sargı Tipleri, Rotor Bariyerleri, Sonlu Elemanlar Analizi.

Öz

Senkron Relüktans Motorlar (SRM'ler) basit yapıları, yüksek verimlilikleri ve nadir toprak mıknatıslarına ihtiyaç duymamaları nedeniyle son yıllarda büyük ilgi görmektedir. SRM'ler, manyetik akıyı rotor içindeki bariyerler aracılığıyla yönlendirerek moment üretir ve bu da onları düşük maliyetli bir alternatif haline getirir. Motorun performansı, stator sargılarının ve rotor bariyerlerinin tasarımına bağlı olarak önemli ölçüde değişebilir. Stator sargı tiplerinin farklı kombinasyonları ve rotor bariyerlerinin sayısı, motorun moment, verimlilik, moment dalgalanması, çıkış gücü, çıkıklık oranı ve bakır tüketimi gibi kritik performans parametrelerini doğrudan etkiler. Bu çalışmada, altı farklı stator sargı tipi ve iki farklı rotor bariyer yapısı (3 ve 4 bariyer) kullanan SRM'ler analiz edilmiştir. Çıkış gücü, verim, moment, moment dalgalanması, çıkıklık oranı, akım faz açısına bağlı d ve q eksen endüktansları, kayıplar ve bakır tüketimi incelenmiştir. Sargı yapılarındaki tam adımlı ve kısaltılmış adımlı konfigürasyonların performans üzerindeki etkisi karşılaştırmalı olarak tartışılmıştır. Ayrıca 3 ve 4 bariyerli rotorların bu parametreler üzerindeki etkisi de değerlendirilmiştir. Bu analizler, motor tasarımında sargı ve rotor konfigürasyonlarının performansı optimize etmek için nasıl kullanılabileceğini ortaya koymayı amaçlamaktadır. SRM'ler çeşitli endüstriyel uygulamalarda enerji verimliliği ve maliyet avantajları sağlayabilir, bu nedenle uygun konfigürasyonun seçilmesi hem ekonomik hem de performans açısından büyük önem taşımaktadır.

Alıntı / Cite

Kartal, E.T., Keskin Arabul, F., (2024). Performance Comparison of Winding Types and Rotor Structure in Synchronous Reluctance Motor, Journal of Engineering Sciences and Design, 12(4), 835-847.

Yazar Kimliği / Author ID (ORCID Number)

Emin Tarık Kartal, 0000-0002-4966-7258
Fatma Keskin Arabul, 0000-0002-9573-8440

Makale Süreci / Article Process	
Başvuru Tarihi / Submission Date	30.09.2024
Revizyon Tarihi / Revision Date	29.10.2024
Kabul Tarihi / Accepted Date	13.11.2024
Yayım Tarihi / Published Date	25.12.2024

[*] İlgili yazar / Corresponding author: fkeskin@yildiz.edu.tr, +90-212-383-5848

PERFORMANCE COMPARISON OF WINDING TYPES AND ROTOR STRUCTURE IN SYNCHRONOUS RELUCTANCE MOTOR

Emin Tarık KARTAL[1], Fatma KESKİN ARABUL[1†]
[1] Yildiz Technical University, Department of Electrical Engineering, Istanbul, Türkiye

Highlights

- This study systematically investigates various stator winding types and rotor barriers configurations for Synchronous Reluctance Motors (SynRMs).
- The findings demonstrate the significant influence of design elements on motor performance.
- The results provide valuable insights for optimizing SynRM configurations in industrial and electric vehicle applications.

Purpose and Scope

The aim of this paper is to examine the stator winding types and rotor barrier structures that affect the performance of SynRMs. This study seeks to enhance understanding of design elements and their implications for motor performance, particularly in applications within the industrial and electric vehicle. Different motor configurations for industrial and electric vehicle applications are evaluated and optimum design recommendations are presented.

Design/methodology/approach

In this study, 2D motor models for 6 different stator winding types and 2 different rotor structures are created by finite element method (FEM) using Ansys-Maxwell software. The parameters required for performance evaluation include torque, efficiency, torque ripple, output power, saliency ratio, copper consumtion in stator, d-q axis inductances depending on current phase angle and total losses. The results of the analysis are presented by comparing different configurations.

Findings

The analyses reveal significant variations in the performance of SynRMs based on different stator winding types and rotor barrier configurations. It is observed that the torque and shaft power increase significantly with the increase in the number of barriers, the rotor structures with 3 barriers have considerably lower torque ripple compared to the structures with 4 barriers, and the winding types have important features in terms of both performance and cost with the analysis results. The WT-3-3 and WT-3-4 configurations offer strong performance for electric vehicles and industrial use, emphasising the significant impact of rotor and stator configurations on motor performance. The WT-3-3 offers a balanced performance with a torque capacity of 290 Nm and an efficiency of 94.80%, while the use of 6.4 kg copper provides a cost-performance advantage; in addition, 12.06% torque ripple improves driving comfort. While WT-3-4 offers higher performance with 311 Nm torque and 95.12% efficiency, torque ripple (16.07%) requires optimisation; this can be addressed in future studies by improving the rotor structure.

Practical implications

The findings indicate that optimizing rotor and stator configurations can enhance the performance of SynRMs, making them more suitable for industrial and electrical vehicle applications. This research can guide future design choices to improve energy efficiency and reduce costs.

Originality

This paper contributes to the literature by presenting a performance analysis of various winding and rotor configurations for SynRMs. The obtained results provide a basis for innovative approaches in motor design.

† Corresponding author: fkeskin@yildiz.edu.tr, +90-212-383-5848

1. Introduction

Synchronous reluctance motors (SynRMs) are gaining attention for their higher reliability, faster dynamic response, and higher efficiency compared to other motor types. SynRMs offer higher efficiency, higher speed range, and higher torque per ampere, making them suitable for medium and low power applications. These motors are known for high flux density per unit volume, low maintenance requirements, and low electromagnetic obstruction (Sivaramkrishnan et al., 2022). SynRMs are designed with a rotor that can be optimized to maximize efficiency on the total operating cycle, considering specific speed and torque profiles. The motors outperform similarly dimensioned induction motors in efficiency, torque, and power density. This make them a step forward compared to permanent magnet motors in terms of cost effectiveness for low power industrial applications. In addition, SynRMs are being considered as a valid alternative to permanent magnet machines, especially for high speed traction applications, due to their robustness, simple structure, and absence of magnets (Grace et al., 2018). These motors have the potential to replace induction, switched reluctance, and permanent magnet motors in various applications, including industrial tools, traction, and low-speed high-power generators (Babetto et al., 2018). Moreover, they are suitable for electric vehicles, offering the potential for more efficient, heavier load, and longer range vehicles, contributing to the adoption of electric vehicles and reducing reliance on fossil fuels. SynRMs are being explored for high-speed traction applications, such as in electric and hybrid electric vehicles, medical equipment, and aerospace (Grace et al., 2018) (Xu et al., 2019). Despite the advantages, SynRMs face challenges related to achieving a good constant power to speed ratio, which is dependent on the mechanical aspects of the design (Grace et al., 2018). Conventional SynRM designs may suffer from high torque ripple and poor power factor, but a redesign of the rotor geometry and optimization of the rotor and stator can significantly improve performance. Nevertheless, the main drawback of reluctance machines is high torque ripple, and achieving a robust geometry for torque ripple reduction is challenging (Bianchi et al., 2013).

The rotor geometry significantly influences the performance of SynRMs by affecting the d-axis and q-axis inductance, saliency ratio, torque ripple, and average torque (Ferrari et al., 2015) (Babetto et al., 2019) (Rezk et al., 2021). The geometry and number of flux barriers are crucial. Optimizing these using finite-element analysis can significantly improve steady-state performance. Different shapes, such as arc and trapezoidal, have been studied for their impact on motor efficiency (Boroujeni et al., 2015). To address mechanical retention and reduce the need for bridges or center posts, a sleeve can be added to the rotor. This improves power density, reduces rotor losses, and minimizes torque ripple (Reddy et al., 2016). The design should aim for high efficiency, maximum torque, and minimal torque ripple. This involves optimizing stator parameters and minimizing air-gap flux leakage. In the study (H. Liu et al., 2018), a 4-pole/36-slot configuration with distributed winding can maximize rated efficiency and minimize air-gap flux leakage, leading to smoother electromagnetic torque. Optimizing the shape and opening of stator slots can reduce torque ripple and improve overall performance. Minimizing slot openings helps in reducing air-gap flux leakage. Asymmetric rotor designs with different flux-barrier geometries in adjacent poles can reduce torque ripple by over 40% without sacrificing average torque. The shape and ends of the flux barriers are crucial in minimizing torque harmonics (Bacco & Bianchi, 2018). Optimizing the rotor geometry, including the number and shape of flux barriers, enhances torque density and efficiency. For instance, considering the current angle during optimization can increase output power by 3.32% and reduce torque ripple by 34.20% (Rezk et al., 2021). The design parameters of rotor geometry that significantly impact SynRM performance include flux-barrier parameters such as angle, width, position, and length, as well as the shape of the barriers, the number of flux barriers per pole, and the thickness of the outer rib. The width of iron parts and barriers along the d and q axis, as well as the angle of end points for each barrier, are optimized to minimize torque ripple and increase average torque (Naeimi et al., 2023). The d-axis and q-axis inductance, which are influenced by rotor geometry, are critical for improving the saliency ratio and overall performance. Proper design can enhance the torque-to-current ratio and steady-state performance. The torque generated by SynRMs is significantly influenced by the difference between direct-axis (L_d) and quadrature-axis (L_q) inductances. Proper alignment of rotor field paths and consideration of magnetic saturations can enhance performance (C.-T. Liu et al., 2015). Studies involving parametric analysis of rotor lamination and flux barriers show that specific geometrical configurations can significantly reduce iron losses and improve efficiency. For example, a design with four flux barriers per pole is found to be optimal (Castagnaro et al., 2019).

The design of stator windings in SynRMs are crucial for optimizing performance, efficiency, and operational flexibility. Various winding configurations, such as conventional double layer (CDL), triple layer (TL), and double triple layer (DTL), are explored. These configurations influence the motor's average torque and torque ripple. For instance, a five phase SynRM with a mixed DTL winding configuration and three rotor flux barriers per pole produced high average torque with low torque ripple (Muteba, 2019). The use of multilayer (ML) AC windings can yield a more sinusoidal stator magnetomotive force (MMF) and shorter end-turn lengths, leading to higher

efficiency and lower torque ripple compared to conventional double layer windings (Kabir & Husain, 2018). SynRMs designed for low speed, high torque applications often explore different rotor pole and stator slot combinations. Integral slot distributed windings (ISDW), fractional slot distributed windings (FSDW), and fractional slot concentrated windings (FSCW) are some of the winding types considered to optimize performance (Artetxe et al., 2018). Advancements in stator winding design for SynRM include the optimization of 5-phase stator dimensions and the use of combined star-pentagon winding to improve machine performance (Tawfiq et al., 2020). The development of a rewinding technique for existing three phase stators to higher numbers of phases has shown enhancements in torque density, torque ripple reduction, and efficiency in SynRM (Tawfiq et al., 2022). Different winding configurations, such as single layer, double layer, and combined star-delta windings, impact the torque density and efficiency. For example, a combined star-delta winding layout can offer a 5.2% enhancement in torque density over a conventional star winding under rated conditions (Ibrahim et al., 2018). Additionally, a combined star-delta-connected stator with permanent magnets in the rotor can significantly increase output torque compared to conventional machines (Ibrahim et al., 2017). The number of stator slots also affects torque performance. Lower stator slot numbers are preferable for higher torque/copper loss ratios, while higher slot numbers are suitable for larger machine scales (Huang et al., 2019). Increasing the stator slot number tends to decrease torque ripple, which is beneficial for smoother motor operation. However, the average torque remains relatively constant when the stator slot number is varied while keeping the pole number the same (Wang et al., 2015).

In this paper, the performance characteristics of SynRMs are systematically examined through the analysis of various stator winding types and rotor barrier configurations. This study aims to contribute to a broader understanding of the impact of design elements on the overall performance of the motors. The remainder of this paper is structured as follows: In the Material and Method section, the modeling and analysis approach using the Finite Element Method (FEM) in Ansys-Maxwell is explained, focusing on industrial and electric vehicle applications of Synchronous Reluctance Motors (SynRMs). Subsequently, the Analysis Results section provides a comparative evaluation of 12 motor configurations, assessing key performance metrics such as torque, efficiency, output power, and phase current. Finally, the Results and Discussion summarizes the findings, highlighting the effects of different winding and rotor configurations on motor performance and recommending optimal design.

2. Material and Method

In this section, the modelling and analyses of the SynRM designed for industrial and electric vehicle applications are be presented comparatively with the results determined for performance evaluation. The models designed in the analyses are created in two dimensions (2D) in Ansys-Maxwell program and analyzed by FEM (Kartal & Keskin Arabul, 2022a). The dimensions, materials, properties and parameters of SynRM are given in Table-1 (Kartal & Keskin Arabul, 2024).

Table 1. Specifications of SynRM.

Stator outer diameter	252 mm
Rotor diameter	154.8 mm
Axial length	152 mm
Air gap length	1 mm
Number of stator slots	60
Number of pole pairs	2
Rated voltage/phase/connection	100 V/3/Y
Rated speed	5010 rpm
Electrical steel	JFE-35JN270

With reference to the motor specifications given in Table 1, the torque, torque ripple, efficiency, output power and saliency ratio determined for the performance evaluation of SynRM in 7 different winding types (WT) and 2 different rotor structures are obtained and presented with the analysis results. It should be noted that, WT-1, WT-2, WT-3 and WT-4 of these winding structures are used in an induction motor designed for electric vehicle applications. (Kartal & Keskin Arabul, 2022b). Figure 1 shows the winding configurations of only single phase of the SynRM models.

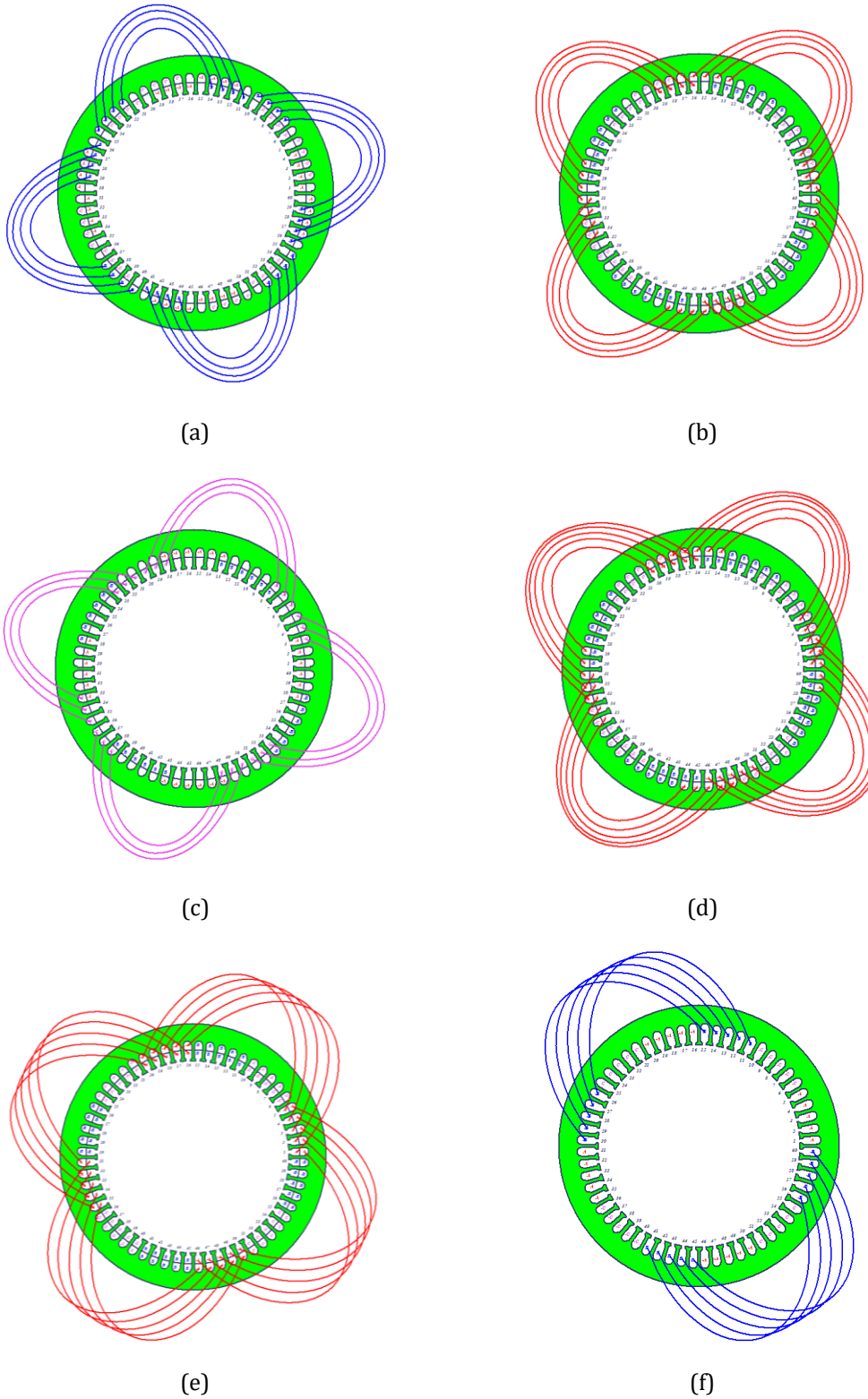

Figure 1. Winding configurations of SynRM models (a) WT-1, (b) WT-2, (c) WT-3, (d) WT-4, (e) WT-5, (f) WT-6.

When it comes to the winding types in consideration with the design parameters of the SynRM given as reference in Table 1, the first one, as presented in Figure 1 (a), WT-1 is a double-layer winding. In this winding structure, the coils are not full-pitch, they are shortened-pitch coils. A symmetrical grouping structure is formed as 4+4 with shortened pitch coils. The coils in the formed groups are not fixed pitch. Coil pitches are 14-12-12-10-8 slots from outside to inside respectively. However, the coils are also not fixed turns. The outermost and the coil with the largest coil pitch is 2-turn and the other coils are single turn. In WT-2, as presented in Figure 1 (b), double-layers of winding are placed in the stator with 60 slots. In this winding structure, the coils are not full-pitch, they are shortened-pitch coils. A symmetrical grouping structure is formed as 4+4 with shortened pitch coils. The coils in

the formed groups are not fixed pitch. Coil pitches are 15-13-13-11-11-9 slots from outside to inside respectively. However, the coils are also not fixed turns. The coil with a coil pitch of 13 slots is 2-turns and the other coils are single turn. In WT-3, as presented in Figure 1 (c), with double layers; in this winding structure, the coils are not full pitch, they are shortened-pitch coils. A symmetrical grouping structure is formed as 3+3 with shortened-pitch coils. The coils in the formed groups are not fixed pitch. Coil pitches are 14-12-12-10 slots from outside to inside respectively. However, the coils are also not fixed turns. The coils with 14 and 12 slots pitch are 2-turns and the other coils are single turn. In WT-4, as presented in Figure 1 (d), with double layers; in this winding structure, the coils are not full pitch, they are shortened-pitch coils. A symmetrical grouping structure is formed as 5+5 with shortened-pitch coils. The coils in the formed groups are not fixed pitch. Coil pitches are 17-15-13-13-11-11-9 slots from outside to inside respectively. In this winding type, the coils are fixed and single turn. In WT-5, as presented in Figure 1 (e), with double layers; in this winding structure, the coils are fixed pitch, and the coils pitch are 15 slots with full (pole) pitch. All coil groups in this winding type are single turn. In WT-6, as presented in Figure 1 (f), single layer windings are placed in 60 slots in the stator. In this winding structure, although the coils are fixed pitch, they have 15 slots with full (pole) pitch. In the conductors in all winding structures designed in the analyses, the conductors used in coils consist of 26 stranded round wires with a diameter of 1.024 mm and a maximum insulation diameter of 0.074 mm are used. In addition, there are two parallel branch in each phase in the stator. Including the slot insulation material, the insulation material between the winding layers and the insulation materials in the slot opening area, the net slot fill is kept at 75%. In addition to these, the rotor structures to be included in the analysis after the winding types are defined are given in Figure-2.

(a) (b)

Figure 2. SynRM rotor structures (a) with 3 flux barriers and (b) with 4 flux barriers.

The isolation ratio, which is the ratio of the barrier air gap length on the q-axis to the rotor lamination length on the same axis, is kept equal and 0.84 for rotor structures with 3 and 4 flux barriers. According to this isolation ratio, the shaft diameter of the rotor structures is determined as 50 mm. In 3-barrier structures, the shortest distance of the first barrier to the shaft radius is 15 mm, and the first, second and third barrier thicknesses from the inside to the outside are 10, 8 and 6 mm, respectively. In 4-barrier structures, the shortest distance of the first barrier to the shaft radius is 10 mm, and the first, second, third and fourth barrier thicknesses from inside to outside are 9, 6, 5 and 4 mm, respectively. In all of the rotor models, the rotor barrier top bridge, which is the closest distance of the barriers to the rotor outer diameter, is determined as 2 mm. Eventually, with all the given design parameters, 2D motor models with 6 different stator winding types and 2 different rotor structures are analyzed and the results are presented.

3. Analysis Results

This section includes the performance analysis of SynRMs based on stator winding configurations and rotor barrier structures. In the motors studied, 12 different combinations are evaluated using six different winding types in the stator (WT-1, WT-2, WT-3, WT-4, WT-5, WT-6) and two different barrier structures in the rotors (3 and 4 barriers). Each combination is investigated with performance parameters such as output power, efficiency, torque, torque ripple, d-q axis inductances depending on current phase angle, total losses, saliency ratio (d-q axis inductance ratio) and copper consumption. In the context of these parameters, the effect of rotor and stator structures on the overall performance of the motor is presented. In particular, the effect of the number of rotor barriers and stator winding type on the output power, efficiency and torque production of the motor is interpreted in detail. Figure 3 shows the electromagnetic torque of SynRM winding models with 3 and 4 flux barriers.

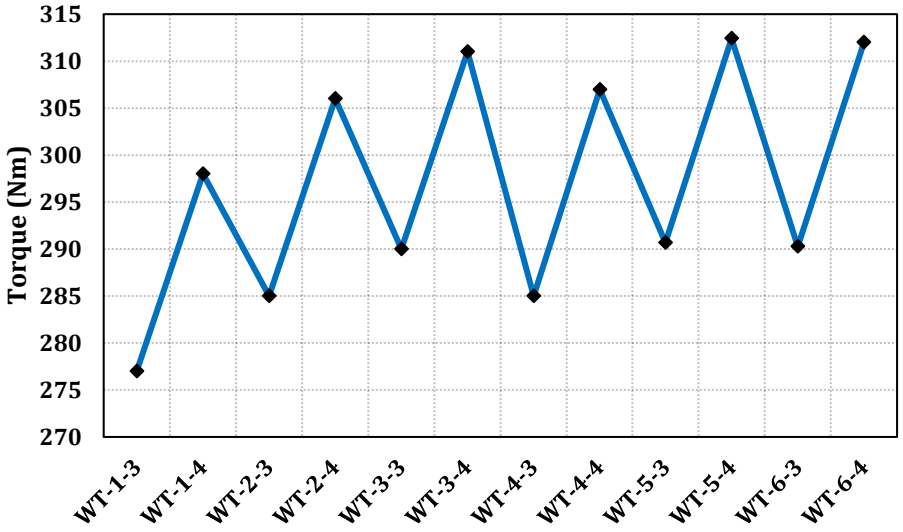

Figure 3. Electromagnetic torque of SynRM winding models with 3 and 4 flux barriers.

First of these, the torque produced by the motor is an important parameter of the motor performance. The Maximum Torque per Ampere (MPTA) control strategy used in the analysis focuses on achieving the highest torque per unit current using the optimum current angle, especially for SynRM in the constant torque region. The basis of this strategy is to improve energy efficiency by optimising the current components required for torque production. In the analyses, the maximum current value determined for all designed motor models is 900 A. Thus, the highest possible torque is obtained with a given current value (900 A). In SynRMs, MPTA control provides maximum torque production by adjusting the current angle according to the rotor structure: 60° for 3-barrier rotors and 65° for 4-barrier rotors. This difference is due to the effect of the number of rotor barriers on the magnetic characteristics of the motor. These different angles are set according to the capacity of the rotor structure to direct the magnetic flux, thus optimising the rotor's contribution to torque production. The 4-barrier structures provide higher torque production with a higher current angle (65°), indicating that increasing the number of barriers has a positive effect on torque.

As can be seen in Figure 3, the maximum torque value belongs to WT-6-4 and WT-5-4 structures with 4 barriers and both of them produce 312 Nm torque. The structure with the lowest torque value is the 3-barrier WT-1-3 model with 277 Nm. In general, it is seen that the structures with 4 barriers provide higher torque in all models. This can be attributed to the reduction of the flux leakage of the motor with the increase in the number of barriers and the more effective orientation of the magnetic flux and the saliency ratio. This difference indicates that 4-barrier structures should be preferred in industrial applications where higher torque is required. Figure 4 shows the shaft power and efficiency of SynRM winding models with 3 and 4 flux barriers.

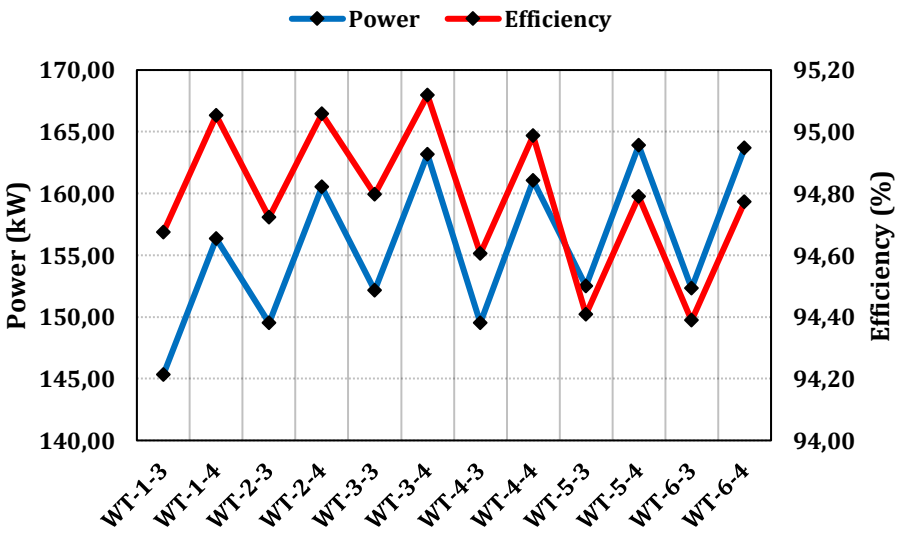

Figure 4. Shaft power and efficiency of SynRM winding models with 3 and 4 flux barriers.

Output power is one of the most important parameters affecting the overall performance of the motor. As shown in Figure 4, In terms of output power, WT-5-4 (163.89 kW) and WT-6-4 (163.68 kW) structures provide the highest value. The lowest power output is observed in the WT-1-3 (145.32 kW) model. Here, it is clearly seen that the structures with 4 barriers keep the output power at a higher level than the structures with 3 barriers. This can be attributed to the fact that with the increase in the number of barriers, the saliency ratio can be kept high and the torque production increases. Therefore, it is advantageous to prefer 4-barrier structures in cases where higher power output is required for electric vehicle applications.

Motor efficiency is an effective indicator of how effectively energy is used. One of the biggest advantages of synchronous reluctance motors is efficiency. Low magnetic leakage and low copper losses allow these motors to operate with high efficiency. As seen in Figure 4, the efficiencies of the WT-1, WT-2 and WT-3 structures above 95% confirm the advantages of synchronous reluctance motors mentioned in the literature. In terms of efficiency, the structure with the highest efficiency is WT-3-4 (95.12%) and the structure with the lowest efficiency is WT-6-3 (94.39%). It is seen that 4-barrier structures generally provide higher efficiency, but in some cases very close efficiency values are obtained with 3-barrier models. This shows that the effect of the number of barriers on the efficiency is not direct and with large differences, but even small differences are important for the management of energy losses. Therefore, in industrial applications with high energy efficiency requirements, it may be recommended to prefer 4-barrier structures that offer efficiency advantages. Figure 5 shows the torque ripple and saliency ratio of SynRM winding models with 3 and 4 flux barriers.

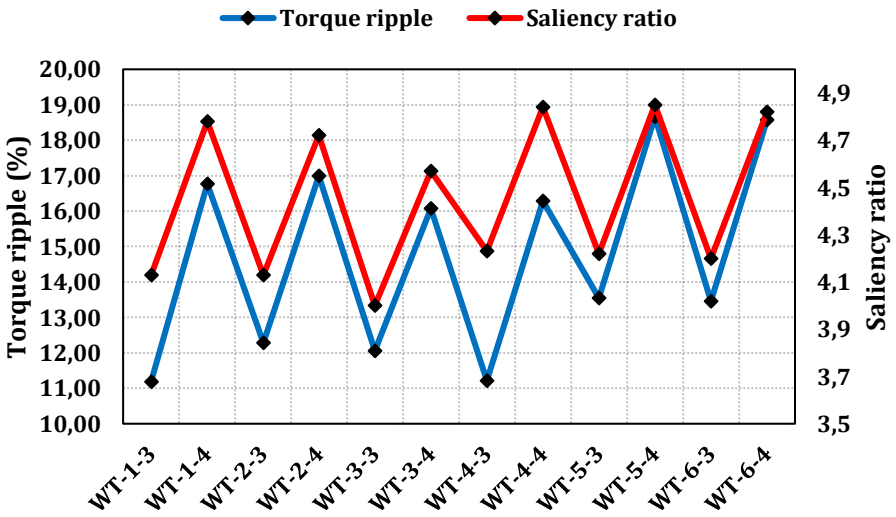

Figure 5. Torque ripple and saliency ratio of SynRM winding models with 3 and 4 flux barriers.

Torque ripple is a critical parameter that affects the proper operation of the motor. As shown in Figure 5, the lowest ripple rate is observed in the WT-1-3 model with 11.19%, while the highest ripple rate is observed in the WT-5-4 model with 18.66%. The results of the analyses show that, in general, 3-barrier structures provide lower torque ripple than 4-barrier structures. This indicates that 3-barrier structures may be more suitable in terms of driving comfort in electric vehicles, while this structure may come to the fore in applications that need to reduce torque ripple.

Saliency ratio is one of the characteristic features of SynRM motors and refers to the ratio of inductances on the d and q axes, determines the torque production capacity of SynRM motors. As shown in Figure 5, a high saliency ratio increases the reluctance torque production of the motor. It is observed that 4-barrier models generally have a higher saliency ratio. Especially WT-5-4 and WT-6-4 models reach high values such as 4.85 in terms of saliency ratio. This indicates that 4-barrier structures cause a more prominent saliency in the magnetic circuit of the motor and positively affect the torque production. In industrial applications, high saliency ratio will be advantageous in processes requiring high torque. However, too high a saliency ratio can cause difficulties in rotor design. Figure 6 shows the total losses and copper weight of SynRM winding models with 3 and 4 flux barriers.

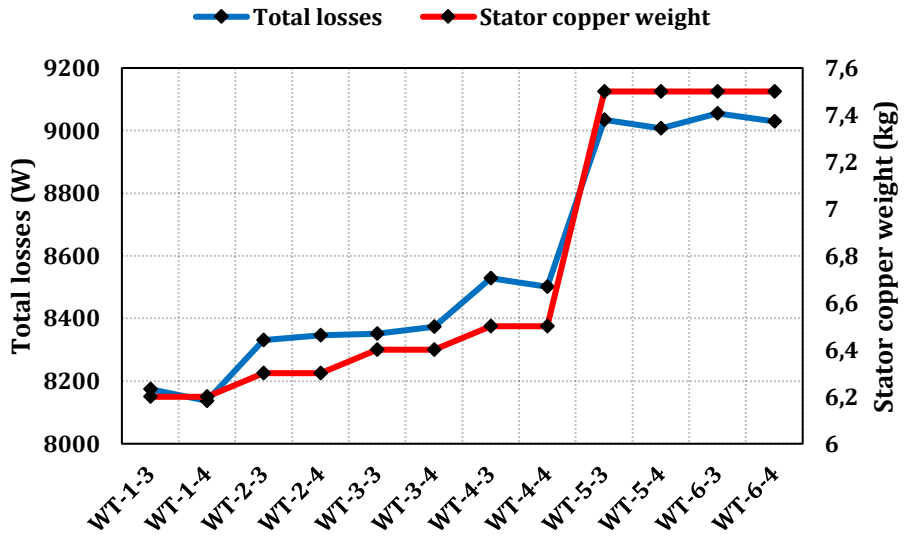

Figure 6. Total losses and copper weight of SynRM winding models with 3 and 4 flux barriers.

As seen in Figure 6, it is seen that the lowest value in total losses is 8174 W in the WT-1-3 model with 3 barriers. The highest total losses are observed as 9029 W in the WT-6-4 model with 4 barriers. These results show that the total losses increase with the increase in the number of barriers. Although the increase in losses may negatively affect the efficiency, the gains in terms of torque and power make these losses tolerable, especially in applications with high performance requirements. The amount of copper is important for the cost and thermal management of the motor. The amount of stator copper varies depending on the winding type, independent of the number of rotor barriers. According to the analysis results, WT-1 and WT-2 winding types have a lower copper consumption with 6.2 and 6.3 kg, respectively, while this amount gradually increases as the winding type increases. WT-5 and WT-6 winding types reached the highest value with 7.5 kg copper consumption in both barrier structures. Increasing the amount of copper, especially in WT-5 and WT-6 winding types, may increase costs while providing higher performance. Therefore, it will be important to pay attention to the winding type selection while making cost optimisation in terms of both performance and cost in industrial and electric vehicle applications. Figure 7 shows the d and q axis inductances depending on the current-phase angle for the WT-1 structures.

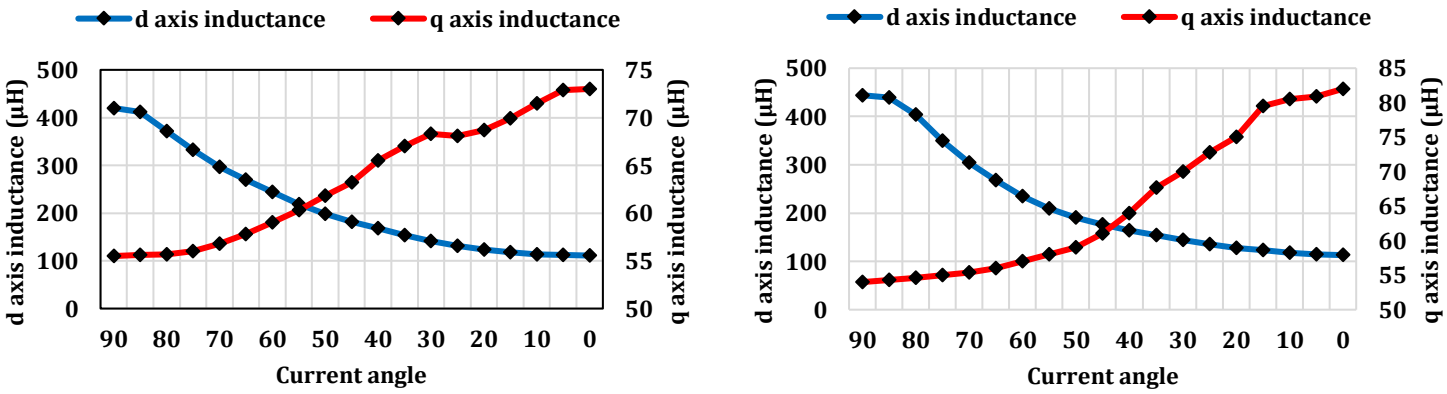

(a) WT-1-3 (b) WT-1-4

Figure 7. d and q axis inductances depending on the current-phase angle for the WT-1 structures.

As can be seen in Figure 7 (a), the saliency ratio of 4.14 in the 3-barrier structure obtained by the analysis results is 244 and 59 µH for d and q axis inductance values, respectively, when the current angle is 60°. In Figure 7 (b), the saliency ratio of 4.79 in the 4-barrier structure is 268 and 56 µH when the current angle is 65° d and q axis inductance values, respectively. Figure 8 shows the d and q axis inductances depending on the current-phase angle for the WT-2 structures.

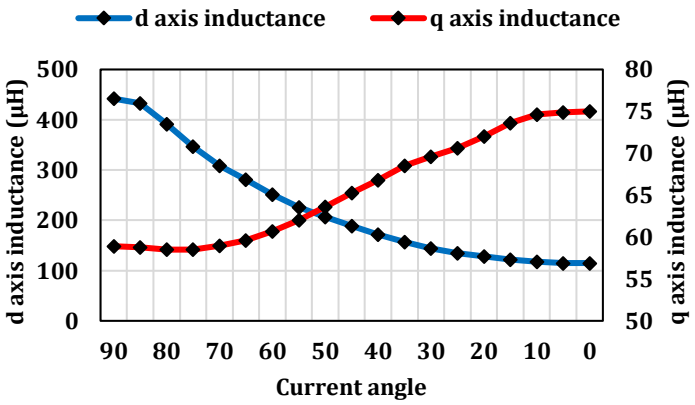

(a) WT-2-3

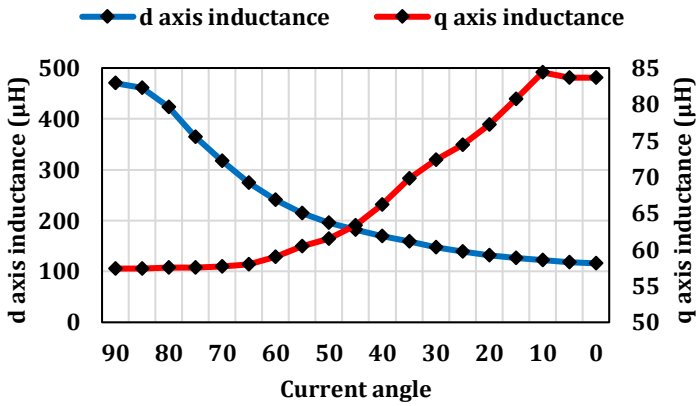

(b) WT-2-4

Figure 8. d and q axis inductances depending on the current-phase angle for the WT-2 structures.

As can be seen in Figure 8 (a), the saliency ratio of 4.14 in the 3-barrier structure obtained by the analysis results is 251 and 60.7 µH for d and q axis inductance values, respectively, when the current angle is 60°. In Figure 8 (b), the saliency ratio of 4.72 in the 4-barrier structure is 274 and 58 µH when the current angle is 65° d and q axis inductance values, respectively. Figure 9 shows the d and q axis inductances depending on the current-phase angle for the WT-3 structures.

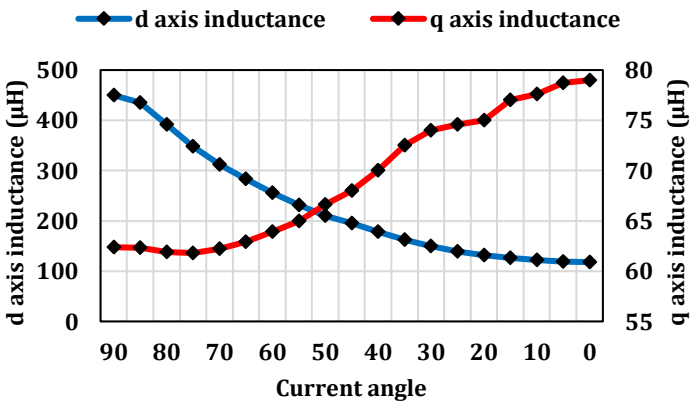

(a) WT-3-3

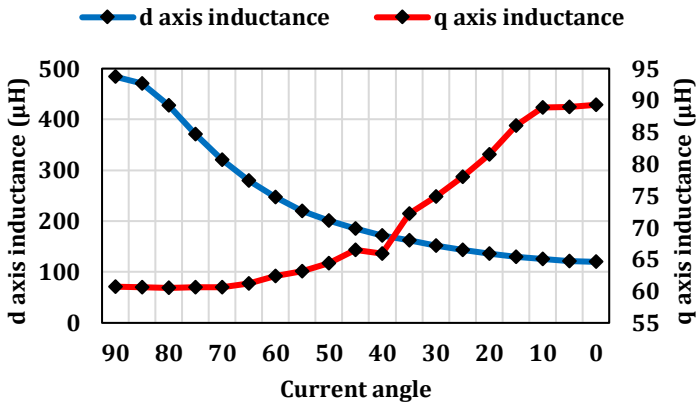

(b) WT-3-4

Figure 9. d and q axis inductances depending on the current-phase angle for the WT-3 structures.

As can be seen in Figure 9 (a), the saliency ratio of 4.01 in the 3-barrier structure obtained by the analysis results is 256 and 63.9 µH for d and q axis inductance values, respectively, when the current angle is 60°. In Figure 9 (b), the saliency ratio of 4.48 in the 4-barrier structure is 280 and 61.2 µH when the current angle is 65° d and q axis inductance values, respectively. Figure 10 shows the d and q axis inductances depending on the current-phase angle for the WT-4 structures.

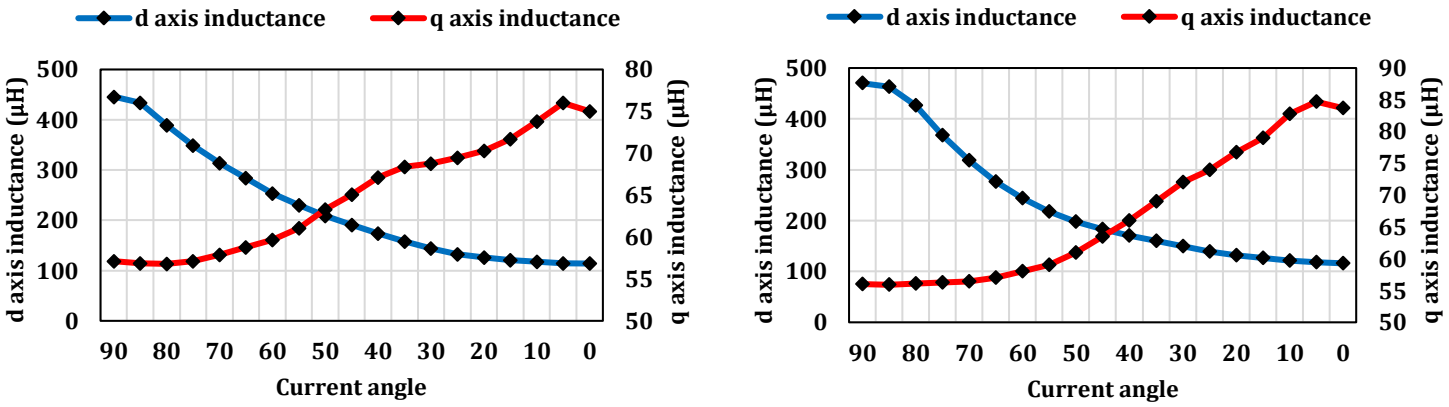

(a) WT-4-3 (b) WT-4-4

Figure 10. d and q axis inductances depending on the current-phase angle for the WT-4 structures.

As can be seen in Figure 10 (a), the saliency ratio of 4.24 in the 3-barrier structure obtained by the analysis results is 253 and 59.7 µH for d and q axis inductance values, respectively, when the current angle is 60°. In Figure 10 (b), the saliency ratio of 4.84 in the 4-barrier structure is 276 and 57 µH when the current angle is 65° d and q axis inductance values, respectively. Figure 11 shows the d and q axis inductances depending on the current-phase angle for the WT-5 structures.

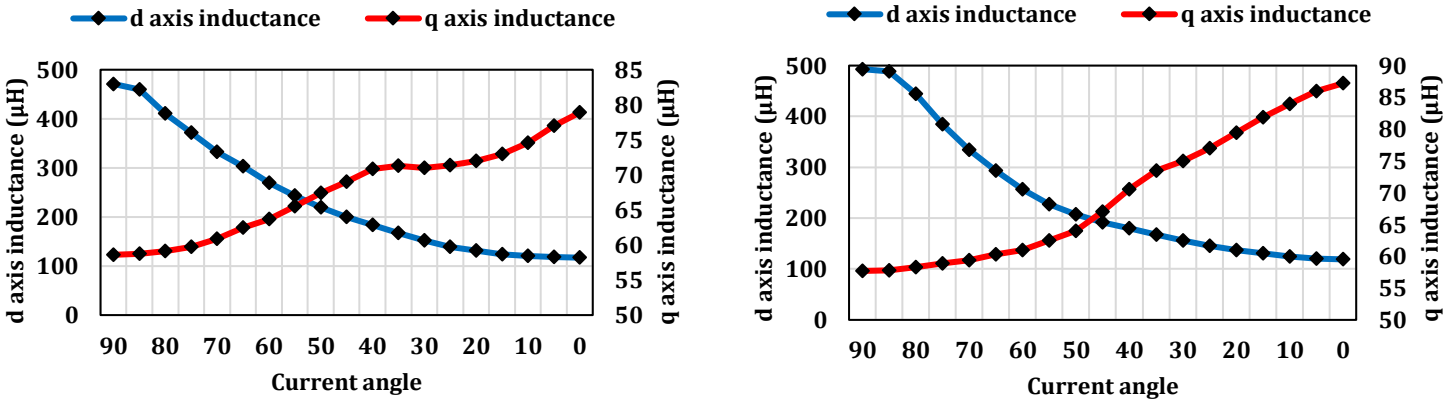

(a) WT-5-3 (b) WT-5-4

Figure 11. d and q axis inductances depending on the current-phase angle for the WT-5 structures.

As can be seen in Figure 11 (a), the saliency ratio of 4.22 in the 3-barrier structure obtained by the analysis results is 269 and 63.7 µH for d and q axis inductance values, respectively, when the current angle is 60°. In Figure 11 (b), the saliency ratio of 4.86 in the 4-barrier structure is 293 and 60.3 µH when the current angle is 65° d and q axis inductance values, respectively. Figure 12 shows the d and q axis inductances depending on the current-phase angle for the WT-6 structures.

4. Conclusion

Consequently, the analyses highlights the significant influence of rotor and stator configurations on motor performance, demonstrating clear differences in key parameters across various designs. WT-3-3 and WT-3-4 configurations are the options that offer strong performance for both electric vehicle applications and industrial use according to the analysis results. Both configurations have similar winding types, but their performances stand out with rotor designs that vary according to different barrier numbers. The WT-3-3 configuration offers balanced performance with a torque capacity of 290 Nm, an output power of 152.14 kW and an efficiency of 94.80%. While the saliency ratio of 4 ensures stable operation of the motor in a wide speed range; 12.06% torque ripple ratio offers a significant advantage especially in terms of driving comfort. The use of 6.4 kg of copper also ensures a balanced design in terms of cost-performance. This configuration is an ideal solution that can provide high performance expectations in electric vehicles while reducing vibration with low torque ripple. The WT-3-4 configuration offers a different flux orientation and control angle with a 4-barrier rotor structure, providing a torque capacity of 311 Nm and an output power of 163.16 kW.

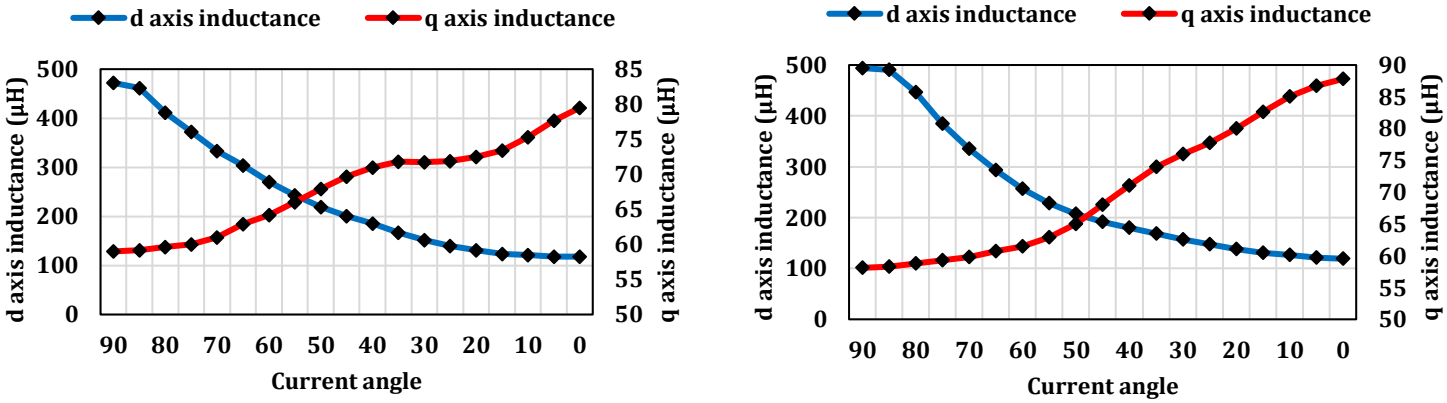

(a) WT-6-3 (b) WT-6-4

Figure 12. d and q axis inductances depending on the current-phase angle for the WT-6 structures.

As can be seen in Figure 12 (a), the saliency ratio of 4.21 in the 3-barrier structure obtained by the analysis results is 270 and 64.2 µH for d and q axis inductance values, respectively, when the current angle is 60°. In Figure 12 (b), the saliency ratio of 4.83 in the 4-barrier structure is 293 and 60.7 µH when the current angle is 65° d and q axis inductance values, respectively.

The efficiency ratio of this configuration is at the highest level of 95.12%, indicating that the motor is efficient in energy utilisation while providing high performance. With a saliency ratio as high as 4.57, the WT-3-4 provides strong reluctance torque production over a wide speed range. However, the torque ripple ratio of 16.07% is slightly higher in the WT-3-4, an issue that needs to be optimised for electric vehicles and industrial applications.

In summary, the WT-3-3 configuration provides a comfortable and efficient use with low torque ripple and balanced output power, while the WT-3-4 configuration stands out with higher torque and output power. Both configurations provide high output power, saliency ratio and efficiency. In future studies, improving the torque ripple by optimising the rotor structure, especially in the WT-3-4 configuration, will contribute to making these configurations more ideal for industrial applications and electric vehicles by increasing performance efficiency.

Conflict of Interest

No conflict of interest was declared by the authors.

References

Artetxe, G., Paredes, J., Prieto, B., Martinez-Iturralde, M., & Elosegui, I. (2018). Optimal pole number and winding designs for low speed-high torque synchronous reluctance machines. *Energies*, *11*(1). https://doi.org/10.3390/en11010128

Babetto, C., Bacco, G., & Bianchi, N. (2018). Synchronous Reluctance Machine Optimization for High-Speed Applications. *IEEE Transactions on Energy Conversion*, *33*(3), 1266–1273. https://doi.org/10.1109/TEC.2018.2800536

Babetto, C., Bacco, G., & Bianchi, N. (2019). Analytical Power Limits Curves of High-Speed Synchronous Reluctance Machines. *IEEE Transactions on Industry Applications*, *55*(2), 1342–1350. https://doi.org/10.1109/TIA.2018.2875663

Bacco, G., & Bianchi, N. (2018). Asymmetric Synchronous Reluctance Rotor Geometry Design: A Practical Approach. *2018 IEEE Energy Conversion Congress and Exposition, ECCE 2018*, 5414–5421. https://doi.org/10.1109/ECCE.2018.8558213

Bianchi, N., Degano, M., & Fornasiero, E. (2013). Sensitivity analysis of torque ripple reduction of synchronous reluctance and interior PM motors. *2013 IEEE Energy Conversion Congress and Exposition, ECCE 2013*, 1842–1849. https://doi.org/10.1109/ECCE.2013.6646932

Boroujeni, S. T., Haghparast, M., & Bianchi, N. (2015). Optimization of flux barriers of line-start synchronous reluctance motors for transient- and steady-state operation. *Electric Power Components and Systems*, *43*(5), 594–606. https://doi.org/10.1080/15325008.2014.984819

Castagnaro, E., Bacco, G., & Bianchi, N. (2019). Impact of Geometry on the Rotor Iron Losses in Synchronous Reluctance Motors. *IEEE Transactions on Industry Applications*, *55*(6), 5865–5872. https://doi.org/10.1109/TIA.2019.2939508

Ferrari, M., Bianchi, N., & Fornasiero, E. (2015). Analysis of rotor saturation in synchronous reluctance and PM-assisted reluctance motors. *IEEE Transactions on Industry Applications*, *51*(1), 169–177. https://doi.org/10.1109/TIA.2014.2326056

Grace, K., Galioto, S., Bodla, K., & El-Refaie, A. M. (2018). Design and Testing of a Carbon-Fiber-Wrapped Synchronous Reluctance Traction Motor. *IEEE Transactions on Industry Applications*, *54*(5), 4207–4217. https://doi.org/10.1109/TIA.2018.2836966

Huang, L., Zhu, Z. Q., Feng, J., Guo, S., Shi, J. X., & Chu, W. (2019). Analysis of Stator/Rotor Pole Combinations in Variable Flux Reluctance Machines Using Magnetic Gearing Effect. *IEEE Transactions on Industry Applications*, *55*(2), 1495–1504.

https://doi.org/10.1109/TIA.2018.2883608
Ibrahim, M. N. F., Abdel-Khalik, A. S., Rashad, E. M., & Sergeant, P. (2018). An Improved Torque Density Synchronous Reluctance Machine With a Combined Star-Delta Winding Layout. *IEEE Transactions on Energy Conversion*, *33*(3), 1015–1024. https://doi.org/10.1109/TEC.2017.2782777
Ibrahim, M. N. F., Rashad, E., & Sergeant, P. (2017). Performance comparison of conventional synchronous reluctance machines and PM-assisted types with combined star-delta winding. *Energies*, *10*(10). https://doi.org/10.3390/en10101500
Kabir, M. A., & Husain, I. (2018). Application of a Multilayer AC Winding to Design Synchronous Reluctance Motors. *IEEE Transactions on Industry Applications*, *54*(6), 5941–5953. https://doi.org/10.1109/TIA.2018.2859033
Kartal, E. T., & Keskin Arabul, F. (2022a). A Comparison between IM and IPMSM with Same Stator Core for EV and Performance Analysis of IPMSM. *European Journal of Science and Technology*, *38*, 165–172. https://doi.org/10.31590/ejosat.1108129
Kartal, E. T., & Keskin Arabul, F. (2022b). Effects of Stator Winding Types and Rotor Slot Geometries on Motor Performance of an Induction Motor for an Electric Vehicle. *9th International Congress on Engineering, Architecture and Design*, 269–276.
Kartal, E. T., & Keskin Arabul, F. (2024). Effects of air gap eccentricity on different rotor structures for PMSM in electric vehicles. *Scientific Reports*, *14*(1), 1–23. https://doi.org/10.1038/s41598-024-68632-z
Liu, C.-T., Luo, T.-Y., Hwang, C.-C., & Chang, B.-Y. (2015). Field Path Design Assessments of a High-Performance Small-Power Synchronous-Reluctance Motor. *IEEE Transactions on Magnetics*, *51*(11). https://doi.org/10.1109/TMAG.2015.2443831
Liu, H., Joo, K. J., Oh, Y. J., Lee, H. J., Seol, H. S., Jin, C. S. J., Kim, W. H., & Lee, J. (2018). Optimal Design of an Ultra-Premium-Efficiency PMA-Synchronous Reluctance Motor with the Winding Method and Stator Parameters to Reduce Flux Leakage and Minimize Torque Pulsations. *IEEE Transactions on Magnetics*, *54*(11). https://doi.org/10.1109/TMAG.2018.2846880
Muteba, M. (2019). Influence of Mixed Stator Winding Configurations and Number of Rotor Flux-Barriers on Torque and Torque Ripple of Five-Phase Synchronous Reluctance Motors. *ITEC 2019 - 2019 IEEE Transportation Electrification Conference and Expo*. https://doi.org/10.1109/ITEC.2019.8790614
Naeimi, M., Nasiri-Zarandi, R., & Abbaszadeh, K. (2023). C- and circular-shaped barriers optimization in a synchronous reluctance rotor for torque ripples minimization. *Scientia Iranica*, *30*(3 D), 1085–1096. https://doi.org/10.24200/sci.2021.57254.5140
Reddy, P. B., Grace, K., & El-Refaie, A. (2016). Conceptual design of sleeve rotor synchronous reluctance motor for traction applications. *Proceedings - 2015 IEEE International Electric Machines and Drives Conference, IEMDC 2015*, 195–201. https://doi.org/10.1109/IEMDC.2015.7409059
Rezk, H., Tawfiq, K. B., Sergeant, P., & Ibrahim, M. N. (2021). Optimal rotor design of synchronous reluctance machines considering the effect of current angle. *Mathematics*, *9*(4), 1–18. https://doi.org/10.3390/math9040344
Sivaramkrishnan, M., Ramkumar, M. S., Subramanian S, S., & Ladu, N. S. D. (2022). A Bridgeless LUO Converter with Glowworm Swarm Optimized Tuned PI Controller for Electrical Applications. *Mathematical Problems in Engineering*, *2022*. https://doi.org/10.1155/2022/2401261
Tawfiq, K. B., Ibrahim, M. N., El-Kholy, E. E., & Sergeant, P. (2020). Performance Improvement of Existing Three Phase Synchronous Reluctance Machine: Stator Upgrading to 5-Phase with Combined Star-Pentagon Winding. *IEEE Access*, *8*, 143569–143583. https://doi.org/10.1109/ACCESS.2020.3014498
Tawfiq, K. B., Ibrahim, M. N., El-Kholy, E. E., & Sergeant, P. (2022). Performance Analysis of a Rewound Multiphase Synchronous Reluctance Machine. *IEEE Journal of Emerging and Selected Topics in Power Electronics*, *10*(1), 297–309. https://doi.org/10.1109/JESTPE.2021.3106591
Wang, K., Zhu, Z. Q., Ombach, G., Koch, M., Zhang, S., & Xu, J. (2015). Torque ripple reduction of synchronous reluctance machines: Optimal slot/pole and flux-barrier layer number combinations. *COMPEL - The International Journal for Computation and Mathematics in Electrical and Electronic Engineering*, *34*(1), 3–17. https://doi.org/10.1108/COMPEL-11-2013-0366
Xu, M., Liu, G., Chen, Q., & Zhao, W. (2019). Design and Key Technology Development of Permanent Magnet Assisted Synchronous Reluctance Motor. *Zhongguo Dianji Gongcheng Xuebao/Proceedings of the Chinese Society of Electrical Engineering*, *39*(23), 7033–7043. https://doi.org/10.13334/j.0258-8013.pcsee.182323